HAL
open science

Experimental study of electrical FitzHugh-Nagumo neurons with modified excitability

Stéphane Binczak, Sabir Jacquir, Jean-Marie Bilbault, Victor B. Kasantsev, Vladimir I. Nekorkin

To cite this version:

Stéphane Binczak, Sabir Jacquir, Jean-Marie Bilbault, Victor B. Kasantsev, Vladimir I. Nekorkin. Experimental study of electrical FitzHugh-Nagumo neurons with modified excitability. Neural Networks, 2006, 19 (5), pp.684-693. 10.1016/j.neunet.2005.07.011 . hal-00584220

HAL Id: hal-00584220

https://u-bourgogne.hal.science/hal-00584220v1

Submitted on 7 Apr 2011

HAL is a multi-disciplinary open access archive for the deposit and dissemination of scientific research documents, whether they are published or not. The documents may come from teaching and research institutions in France or abroad, or from public or private research centers.

L'archive ouverte pluridisciplinaire **HAL**, est destinée au dépôt et à la diffusion de documents scientifiques de niveau recherche, publiés ou non, émanant des établissements d'enseignement et de recherche français ou étrangers, des laboratoires publics ou privés.

Experimental study of electrical MFHN neurons

S. Binczak[a], S. Jacquir[a], J.M. Bilbault[a], V.B. Kazantsev[b] and V.I. Nekorkin[b]

a) Laboratoire LE2I, CNRS UMR 5158,
Aile des Sciences de l'Ingénieur,
Université de Bourgogne,
BP 47870, Dijon Cedex, France
b) Institute of Applied Physics of RAS,
46 Uljanov str.,
603950 Nizhny Novgorod, Russia

June 23, 2004

Abstract

We present an electronical analogue circuit modelling a FitzHugh-Nagumo neuron with a modified excitability. To characterize this basic cell, the bifurcation curves between stability with excitation threshold, bistability and oscillations are investigated. An electrical circuit is then proposed to realize an unidirectional coupling between two cells, mimicking an inter-neuron synpatic coupling. In such a master-slave configuration, we show experimentally how the coupling strength control the dynamic of the slave neuron, leading to frequency locking, chaotic behavior and synchronization. These phenomena are then studied by phase map analysis. The architecture of a possible neural network is then described introducing different kind of coupling between neurons.

1 Introduction

As biological neurons have been well studied over the previous century, there is nowadays a strong interest in realizing electrical networks to reproduce the activity of biological neurons. Accurate models are usually used to describe biological neural network, such as Hodgkin and Huxley (HH) [1], and are subject to intensive studies [2, 3] in engineering science. Nevertheless, mathematicians often study the 2-component FitzHugh-Nagumo (FHN) model [4, 5], as a simplified version of the HH one. This set of equations leads indeed to analytical studies, enlightening the nonlinear dynamical mechanisms generating complex patterns in the neural information process [6].

Although these differential equations are used to model the nerve membrane [6, 7], we suggest to describe overall activity of the neuron by them. In this reductive approach, we propose an experimental electronic implementation of a neuron based on the FitzHugh-Nagumo (FHN) equation with modified excitability to conceive the electronic MFHN neuron [8].

In the first part, the electronic neuron is presented and characterized by its experimental bifurcation curves, showing that this MFHN circuit leads to complex dynamics of travelling waves [9, 10] emerging from saddle homoclinic loop bifurcations.

In the second part, we use the MFHN circuit as a basic cell to realize a master-slave configuration. Two cells are coupled in an unidirectional manner, which would correspond to two neurons coupled synaptically. After the presentation of the electronic circuit giving this coupling, we discuss the experimental conditions for which the master dynamics controls the

excitability of the slave neuron leading to a shift of bifurcation curves, a variation of interspike frequencies or a phenomenon of intermittency route to chaos. Finally, we present the architecture of a possible experimental network including different electrical realizations of neuronal coupling.

2 Experimental description of one cell

2.1 Electrical circuit

The nonlinear circuit, as sketched in Fig. 1, can be described as follows: Part (A) is a parallel association of three different branches, two of them being resistive and commuted by silicium diodes ($Vd = 0.6\ V$) while the third one is a negative resistor obtained with an operational amplifier. Due to diodes' commuting behaviour, the resulting I-V characteristic is nonlinear and can be modelled by a cubic polynomial function for an appropriate set of parameters so that

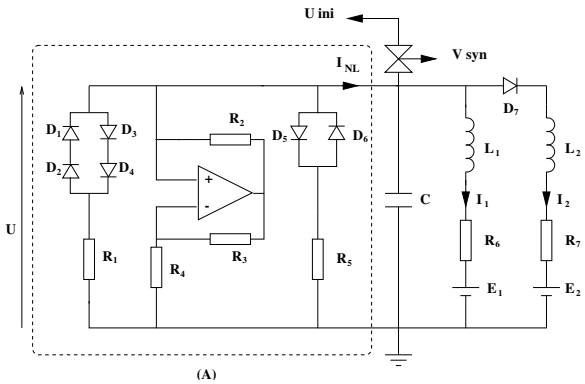

Figure 1: Diagram of the nonlinear circuit

$$I_{NL} = f(U) = \frac{1}{R_0}\left[U - \frac{\gamma^2 U^3}{3}\right], \qquad (1)$$

where U and I_{NL} are respectively the voltage and the corresponding current. The parameters R_0 and γ are obtained by a fitting approximation, e.g. by least mean square's method. As illustrated in Fig. 2, we obtain a good match between experimental results and equation (1) by setting $R_0 = 1010\ \Omega$ and $\gamma = 1.138\ V^{-1}$. This nonlinear resistor is in parallel

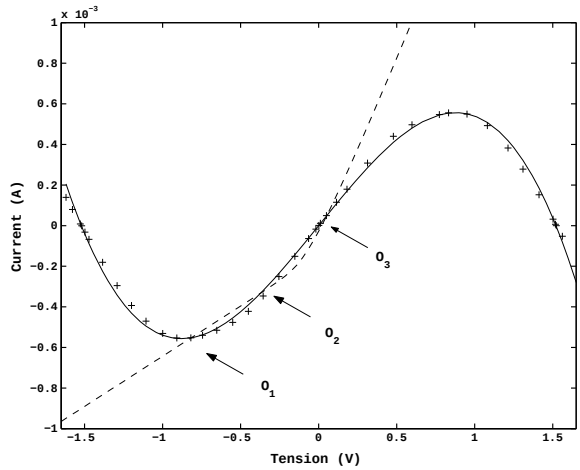

Figure 2: Experimental I-V characteristic (+ symbols) of part (A). Continuous line: $I_{NL} = f(U)$ from eq. (1) with $R_0 = 1010\ \Omega$ and $\gamma = 1.138\ V^{-1}$. Dashed line: Experimental I-V characteristic $I_1 + I_2 = h(U)$ with $R_6 = 2021\ \Omega$, $R_7 = 690\ \Omega$, $L_1 = 10.2\ mH$, $L_2 = 3.5\ mH$ and $E_1 = 0.4\ V$

with a capacitance and two branches in parallel including inductances, resistances and voltage sources, one of them being commuted by a silicium diode so that setting the conditions $\frac{R_6}{L_1} = \frac{R_7}{L_2}$, $E_2 = -Vd$, and using a piecewise linear I-V description for diode D_7, $I_2 = 0$ if $U < 0$. Therefore, using Kirchhoff's laws, the system of equations can be expressed in a normalized way by :

$$\begin{cases} \dfrac{dV}{d\tau} = \left[V - \dfrac{V^3}{3}\right] - W \\ \dfrac{dW}{d\tau} = \varepsilon\Big[g(V) - W - \eta\Big] \end{cases} \qquad (2)$$

Where $V = \gamma U$ and $W = \gamma R_0(I_1 + I_2)$ correspond, in biological terms, to the membrane voltage and the recovery variable; $\tau = \frac{t}{R_0 C}$ is a rescaled time, $\varepsilon = \frac{R_0 R_6 C}{L_1}$ the recovery parameter and $\eta = \gamma \frac{R_0}{R_6} E_1$ a bifurcation parameter. $g(V)$ is a piecewise linear

function, $g(V) = \alpha V$ if $V \leq 0$ and $g(V) = \beta V$ if $V > 0$ where $\alpha = \dfrac{R_0}{R_6}$ and $\beta = \dfrac{L_1 + L_2}{L_2}\dfrac{R_0}{R_6}$ control the shape and location of the W-nullcline [8].
Note also that the initial condition U_{ini} can be loaded in the neuron via an analogue commutator controlled by a periodic signal V_{syn}.

2.2 Experimental bifurcation curves of MFHN circuit

This section presents different dynamics of the MFHN neuron [8]. In the case, $\alpha = \beta$, the system corresponds to the standard FitzHugh-Nagumo (FHN) equation where the recovery variable is driven by a linear function of the "membrane voltage". In the general case $\alpha \neq \beta$, equation (2) exhibits much more complex dynamics. The phase portrait is very similar to the one occurring from the modified Morris-Lecar (ML) equations [11, 7] proposed to model barnacle muscle fibres and pyramidal cells. Considering the case $\alpha = 0.5$ and $\beta = 1.96$, experimental bifurcation curves in the parameter plane (η,ε) is presented in Fig. 3. Several results are to be distinguished de-

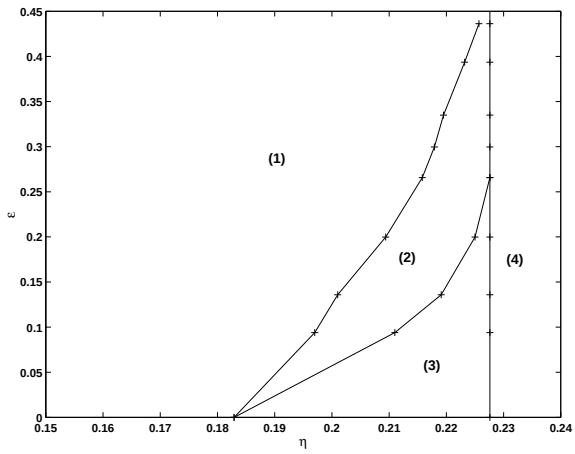

Figure 3: Experimental bifurcation curves in the dimensionless plane (η, ε).

pending on the location of the nullcline points and on initial conditions. In domain (1), the systeme has one stable and unstable fixed point, while one point is a saddle. Then, if a perturbation of the rest state, O_1, is large enough so that it lies between the points O_2 and O_3, the system responds with an excitation pulse, as illustrated in Fig. 4. The upper inset shows

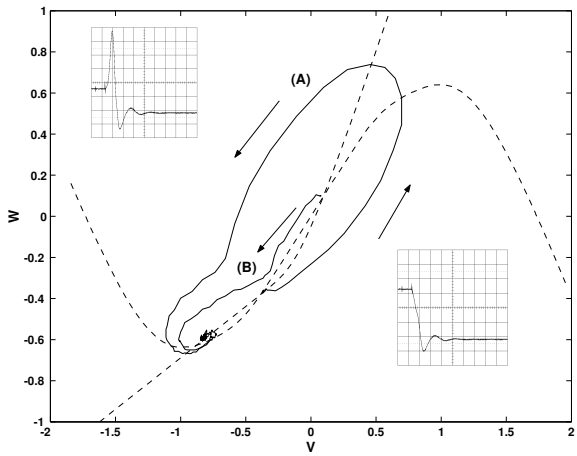

Figure 4: Dimensionless phase plane (V,W) showing stability with excitation threshold corresponding to domain (1) of Fig.3 with $\eta = 0.19$ and $\varepsilon = 0.2$ ($E_1 = 0.332\ V$ and $C = 1\ nF$). Insets: Excitation pulse (upper inset); perturbation reaching resting state (lower inset). Parameters of insets: abscissa 20 $\mu s/div$; ordinate 225 mV/div.

an excitation pulse while the bottom one shows a perturbation reaching the resting state; the main figure gives the respective experimental phase portrait for the both cases. Domain (2) corresponds to the bistability case characterized by the existence of a stable fixed point and a stable limit cycle that has appeared from a big homoclinic loop bifurcation. Then, the model exhibits oscillations if the perturbation is large enough, as illustrated in Fig. 5. The inset shows a spiking train of pulses corresponding to the limit cycle in the experimental phase portrait. Otherwise, it decays to the rest state. In domain (3), the fixed point looses stability via a subcritical Andronov-Hopf bifurcation and only oscillations occur in the model, which are similar to the spiking train of pulses. Note that in the region (2), another saddle homoclinic loop bifurcation has taken place leading to a small unsta-

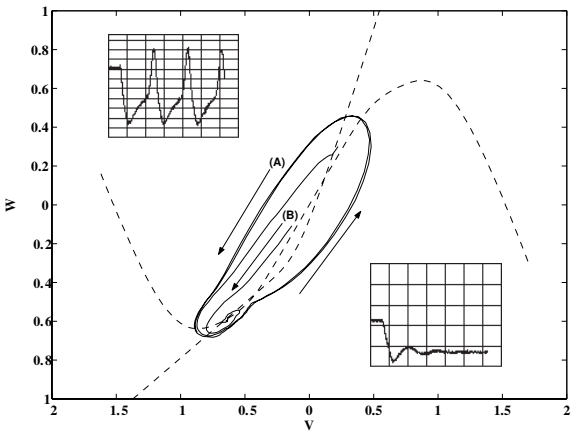

Figure 5: Dimensionless phase plane (V,W) showing bistability corresponding to domain (2) of Fig. 3 with $\eta = 0.226$ and $\varepsilon = 0.2$ ($E_1 = 0.3981\ V$ and $C = 1\ nF$). Inset: Spiking train of pulses corresponding to limit cycle in experimental phase portrait. Parameters of inset: abscissa 20 $\mu s/div$; ordinate 195 mV/div.

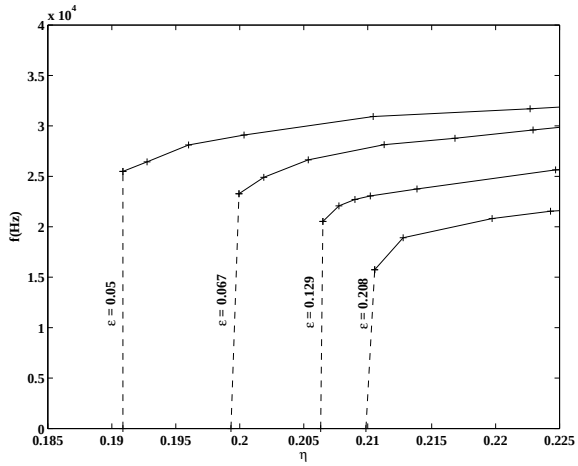

Figure 6: Frequency of an oscillating neuron in function of the parameters η and ε. The dot lines correspond to a jump from the resting state to the oscillating one.

ble limit cycle near the fixed point. Note also that, contrary to standard FHN, arbitrarily long interspike intervals can be found theoretically, as the two lower equilibrium points are merging. Finally, in domain (4), a single unstable fixed point exists leading to oscillations. In domains (2) and (3), the frequency of the oscillations is controlled by the parameters η and ε, leading to a wide range of values, as illustrated in Fig. 6.

In the following section, we study the dynamical behaviour of a network composed of two neurons connected unilaterally.

3 Unidirectional coupling of two cells

The neurons communicate mainly between them through specialized devices called synapses via chemical messages. The chemical synapse transmits the impulse unidirectionally. Therefore, it is interesting to conceive and to realize an electrical circuit including the same features as the synaptical coupling. We present in Fig. 7 the unidirectional coupling between two cells leading to a master-slave configuration where $N_i (i = 1, 2)$ are described by the circuit of Fig. 1. Let us introduce D the coupling parame-

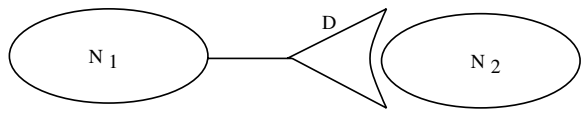

Figure 7: Coupling between two cells N_1 and N_2.

ter (synaptic strength). Its circuit, as illustrated in the Fig. 8, includes an adder-inverter, an inverter and then a follower. $U1$ (resp. $U2$) is the voltage capacitor of the cell $N1$ (resp. $N2$). The value of the resistor R is fixed to 100 $k\Omega$, which is large compared to the other components so that the current going though $2R$ is negligible, $Ra = 10\ k\Omega$, while Rc is a detuning parameter which allows to control the coupling parameter value. Note also that the initial condition can be loaded in the neuron via an analogue commutator controlled by V_{syn}. Although it is usual to study a system with normalized variables, it

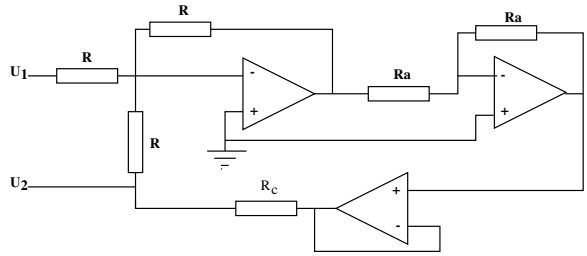

Figure 8: Unidirectional coupling circuit.

is more convenient to describe electrical circuits with experimental variables. Therefore, we will keep both variables (as normalized V_1 and experimental U_1) in the following of this paper. Using Kirchoff's laws, the normalized equations corresponding to the coupling between two MFHN neurons in a master-slave configuration can be expressed by:

$$\begin{cases} \dfrac{dV_i}{d\tau} = \left[V_i - \dfrac{V_i^3}{3}\right] - W_i + DV_1\delta_{2,i} \\ \dfrac{dW_i}{d\tau} = \varepsilon_i\Big[g(V_i) - W_i - \eta_i\Big] \end{cases} \tag{3}$$

with $i = \{1, 2\}$, $D = \frac{R_0}{R_c}$, and where $\delta_{2,i}$ is a Kronecker symbol, so that $\delta_{2,1} = 0$ and $\delta_{2,2} = 1$.
Therefore, the two neurons are coupled so that a part of current weighted by D via R, and generated by N_1 is included in N_2. The two neurons are initially set to voltage U_1ini and U_2ini, due to the analogue commutators controlled by voltage V_{syn}. When the initial conditions are loaded, these commutators are switched off while the two neurons are connected via a third commutator controlled by $\overline{V_{syn}}$. Note that the time delay between the two neurons has not been taken into account in this circuit, a master-slave configuration rendering it unnecessary.

3.1 The master in a resting state

When the voltage is so that V_1 is constant (the cell N_1 is in a resting state), the dynamics of the slave cell is given by eqs. (2) with effective bifurcation parameter

$$\bar{\eta_2} = \eta_2 - DV_1^* \ , \tag{4}$$

where $V_1^* < 0$ is the voltage at stable resting state of the master. Therefore, it implies a modification of the excitability of the cell N_2 corresponding to a shift in the (η, ε) plane illustrated on Fig. 9. The parameters are taken so that, when $D = 0$, the master neuron N_1 lies in domain (1), while the slave neuron N_2 is in domain (3) and generates a spiking train of pulses. When the unilateral coupling is increased and reaches a critical value, the neuron N_2 ceases to oscillate and stays in the resting state, meaning that the slave neuron has been moved from domain (3) to domain (1) of Fig. 3. This ability of neuron N_1 to inhibit neuron N_2 corresponds to the shift predicted by equation (4): As $V_1^* < 0$, increasing D implies to increase $\bar{\eta_2}$ and therefore the bifurcation curves of Fig. 3 are translated along abscissa, while the value of η_2 defined by the electrical parameters of neuron N_2 has not been changed. This result suggests that, for a defined activity of a slave neuron, the strength of this unilateral coupling should be above a critical value to give to the master neuron the control on the slave neuron. In Fig. 9, experimental values $(D, \bar{\eta_2})$

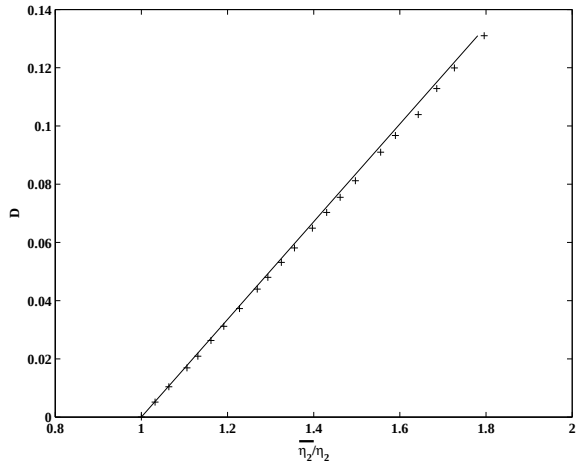

Figure 9: Shifted bifurcation curve of the slave neuron N_2 between domains (1) and (3). Parameters: Master neuron N_1: $\alpha_1 = 0.5$, $\beta_1 = 1.96$, $\epsilon_1 = 0.01$, $\eta_1 = 0.108$ leading to $V_1 = -1.05$ (i.e. $U_1 = -921mV$). Slave neuron N_2: $\alpha_2 = 0.5$, $\beta_2 = 1.96$, $\epsilon_2 = 0.01$

correspond to the shifted bifurcation curve between domains (1) and (3) of the neuron N_2 with $\varepsilon_2 = 0.01$ and when the master neuron N_1 lies in domain (1) in a resting state so that $V_1^* = -1.05$. Comparison shows a good match between experimental results (+) and equation (4) (continuous line), validating the unilateral coupling circuit.

3.2 The master in a spiking regime

In this section, we present some results when the master is in domain (2) or (3) and oscillates. As V_1 is varying in time, we cannot express a simple relationship between the parameters of neuron N_2 and V_1, as in equation (4). Nevertheless, oscillations of neurons N_1 let V_1 be alternatively positive and negative, which implies that the bifurcation curves of neurons are translated along the abscissa in the plane (η, ϵ) in a periodic manner (the position of saddle points of the cell N_2 is moved periodically). Thus, the slave neuron N_2 initially situated in the vicinity of a bifurcation curve may be able to cross sometimes this curve and develop a different dynamical behaviour.

Therefore, the master neuron can control the dynamic of the slave one depending on either its intrinsic behaviour or on the coupling parameter D.

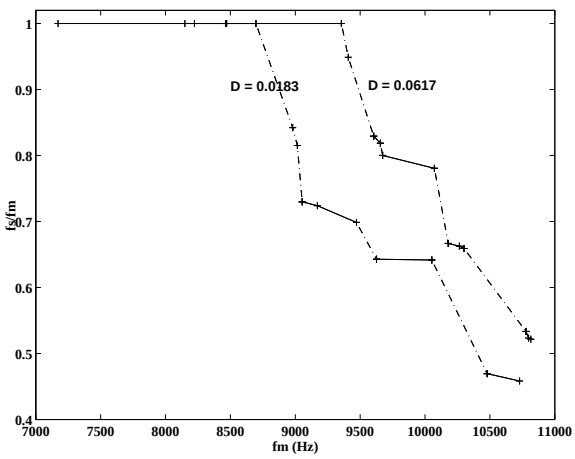

Figure 10: Normalized eigen interspike frequency f_s/f_m in function of f_m for two values of D. Parameters : $\varepsilon_1 = 0.1934$, $\varepsilon_2 = 0.1938$ and $\eta_2 = 0.2163$.

The influence of the frequency f_m of the oscillating master neuron on the dynamical behaviour of the slave neuron is illustrated in Fig. 10, where the normalised eigenfrequencies f_s/f_m with f_s, frequency of the oscillating slave neuron, are plotted in function of f_m (given by η_1 as presented in Fig. 6) for two values of D.

Initially, the slave uncoupled neuron is so that it lies in domain (2) at the resting state, while the master neuron is oscillating.

In both cases, synchronization occurs for small values of f_m, the locking range being wider for stronger D. When f_m is above a critical value depending on the coupling, chaotic behavior emerges, separating frequency locking plateaus. This result suggests that the excitability of the master neuron controls the dynamics of the slave neuron. It is interesting to note that chaotic response is observed in a wide range of frequencies, which in is accordance with numerous biological observations [12].

It also suggests that the coupling parameter D changes the behaviour of the slave neuron.

Note that D is the parameter controlling the interaction strength. Then changing D mimics variable "plasticity" of the synaptic interaction. We fix the

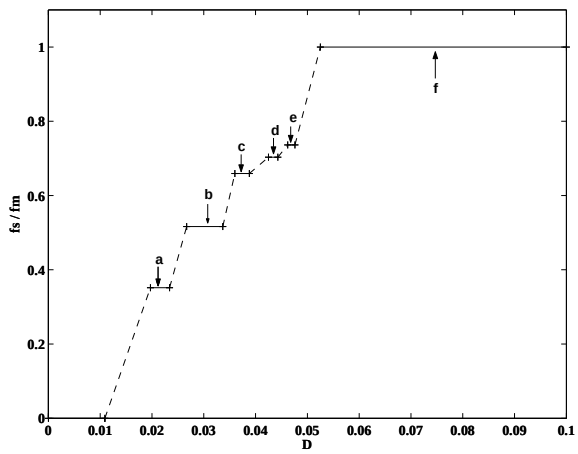

Figure 11: Normalized eigen interspike slave frequency f_s by interspike master frequency f_m versus D with $\epsilon_1 = 0.1934$, $\epsilon_2 = 0.1938$, $\eta_1 = 0.2527$ and $\eta_2 = 0.2262$.

master frequency (hence fix the incoming spike message) and show how the parameter D controls the response dynamics of the slave neuron (Fig. 11 and 12)

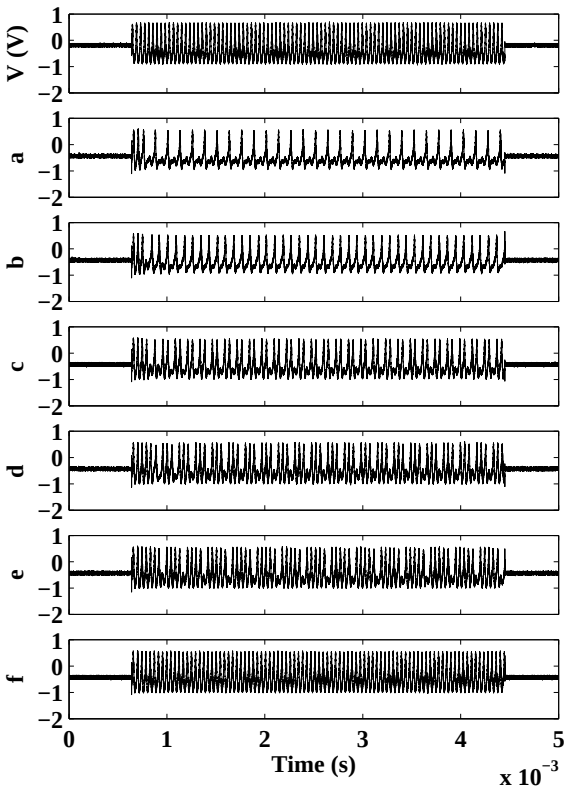

Figure 12: Temporal evolution of experimental voltage U_2 for different values of D corresponding to cases $(a-f)$ of Fig. 11. Voltage of the master neuron N_1 is shown on top. Abscissa : 0.5 ms/div; ordinate: 1 V/div.

Figure 11 shows normalized spike frequency locking diagram. Spike frequency locking is defined as the ratio $N:M$ where M is the number of master spikes in a certain time window and N is the number of successive response spikes of the slave neuron. Figure 12 (a-f) illustrates the spike trains corresponding to plateaus (a-f) in Fig. 11. With increasing value of D (from a to f) the number of response spikes increases reaching its maximum value $f_s/f_m = 1$ (Fig. 12 (f) to be compared with the curve at the top corresponding to master oscillations). This corresponds to $1:1$ spike synchronization mode when the slave repeats the incoming spike message. The frequency

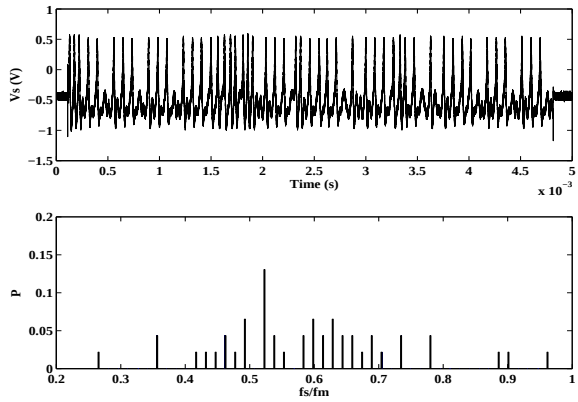

Figure 13: Chaotic signal in the case where $D = 0.0535$. Abscissa : $5s$ per division; ordinate : 1 V per division.

locking plateaus are separated by chaotic sequences, represented in dot lines in Fig. 11.

An illustration of a chaotic signal is given in Fig. 13 for $D = 0.02775$. The corresponding probability of normalized interspike slave frequency fs/fm shows that in a chaotic regime, the interspike frequencies are widely distributed, indicating that the response spike timing can be very complex. In particular, the sequence has variable inter-spike periods which, however, should be associated with the initiating master spike sequence. Then, we define the relative spiking phase variable, ϕ_n, characterizing relative time (phase) shift between a master spike and the following response spike [14]. The definition of ϕ_n is illustrated in Fig. 14. We take it as

$$\phi_n = (t_n^s - t_n^m)/T, \tag{5}$$

where t_n^s and t_n^m are the spike peak times of the slave and master unit, respectively, T is the master oscillation period and n is the number of successive slave spike in the response sequence. Figure 15 illustrates the spiking phase bifurcation diagram obtained experimentally. Here the value of ϕ_n, $n = 1, 2, 3, \ldots$

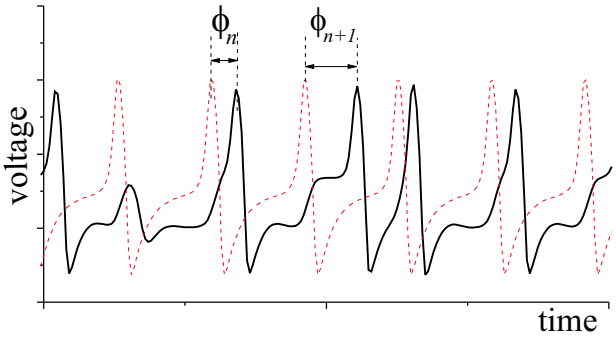

Figure 14: Qualitative view of superimposed master and slave time series shown by dashed and solid curves, respectively. The spiking phase, ϕ_n, is defined as a time shift between master and slave oscillations peaks.

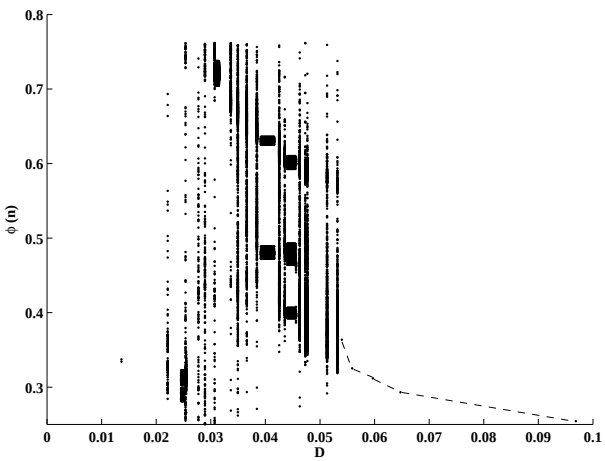

Figure 15: Experimental spiking phase bifurcation diagram. ϕ^* points are linked by the dot line

computed over master-slave experimental traces (Fig. 12,13) are plotted versus coupling coefficient D. It appears that for $1:1$ frequency locking mode the phase tends to a single fixed point ϕ^*. This value accounts the phase shift in the synchronized spiking sequence shown in Fig. 13 (f). Note that for more complicated frequency locking modes the phase shift is described either by stable fixed points with $m < \phi^* < m+1$, where m is number of "integrated" master spikes to get a response, or by stable periodic orbits of a certain period. Note also that transition to chaos suddenly occurs with decreasing D. In this case the spiking phases "fill" some interval with arbitrary changing values from spike to spike. To characterize the phase sequences we calculate the phase map diagrams in the (ϕ_n, ϕ_{n+1})-plane (Fig. 16). For $1:1$ locking mode the map has one stable fixed point ϕ^* (for instance, $\phi^* = 0.5$ in Fig. 16 (c)). With crossing to the chaotic region the fixed point disappears and the phase starts to oscillate. Note the points are located near some curve in the (ϕ_n, ϕ_{n+1})-plane. Then the phase dynamics can be approximately described by a 1D phase map, $\phi_n \rightarrow \phi_{n+1}$. Note also that the map curve goes very close to the bisector line, $\phi_{n+1} = \phi_n$. Then, the dynamics occurs as follows. The phase shift between master and slave spikes is slowly increasing while evolving near the bisector line. Then, the phase jumps out of the $1:1$ response region. After one or a few oscillations it returns back to the $\phi_{n+1} \approx \phi_n$ - region (Fig. 16 (b)). Such behavior indicates the intermittency chaotic dynamics of the phase variable. Note that the jumps corresponds to the appearance of "missed" spike in the response sequence relative to the master oscillations. More complex intermittency behavior with increasing number of jumps, indicating different missed spike numbers, are shown in Fig. 16 (a).

Thus the response spike sequences obtained in the master-slave neuron model can be associated with spiking phase sequences which can be thought as a kind of neuronal "code". The "code" is tuned by the values of interaction coefficient, D. The relative spiking phase represents biologically relevant characteristics of real neuron dynamics. For example, oscillation phase processing plays a crucial role in object tracking by hippocampus neurons [13].

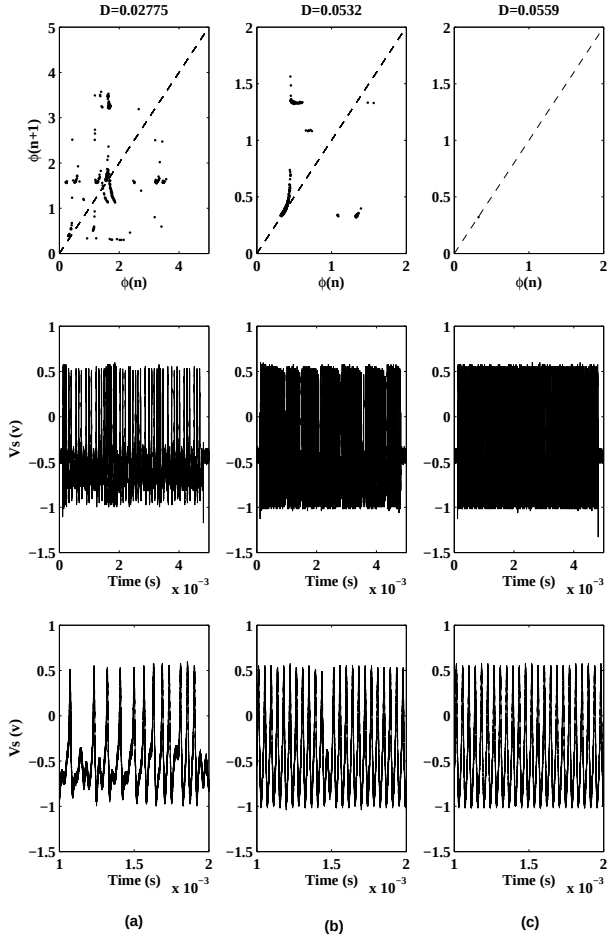

Figure 16: Experimental (ϕ_n, ϕ_{n+1})-plane. The phase map are shown at the top of the figure. The corresponding temporal signals are given below. Zoom of each signal is presented at the bottom of the figure.

4 Architecture of the neural network

The previous study allowed us to validate the experimental setup where two neurons where connected unilaterally: The results have been indeed confirmed by numeral simulations of eq. (1) using a fourth order runge-kutta algorithm. Therefore, it is interesting to increase the size of the network to realize complex configuration mimicking small assemblies of neurons. In this reductive point of view, the neurons can be connected via unilateral coupling, as presented previously or via bidirectional coupling, which would correspond to electrical synapses (gap junctions). The first mentioned coupling is improved to generate either inhibitory or excitatory connection (see Fig. 17) such as the current flowing from neuron n to neuron m can be expressed by $I = D(V_n - Vc)$ where D can be either positive and negative and where V_c is the voltage of the neuron n at its resting state. The

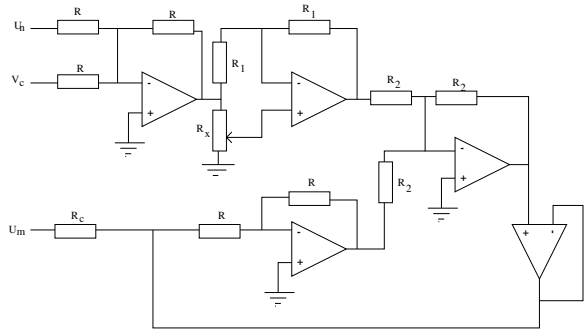

Figure 17: Electrical excitatory or inhibitory coupling.

bidirectional circuit is simply obtained by detuning resistors.
Furthermore, an integration of such a circuit using inductor-like components could be realized, giving this opportunity of very large scale network.

5 Conclusion

We have presented analog electronic circuit implementing MFHN mathematical model. It reproduces

the key features of neuron dynamics including excitability, oscillatory dynamics and bistability. We have experimentally investigated the main bifurcations of the model leading to oscillatory and excitable behavior. We have analysed a simple neuron network architecture with two cells in master-slave configuration, *e. g.* unidirectional coupling. We have shown that the intervals between successive spikes can be chaotic and depends on the intrinsic behaviour of the master neuron and on the coupling strength. The various dynamics of the slave neuron can be reached by detuning D, which could be useful in the point of view of neuronal plasticity.

Acknowledgments

This research was supported in part by Russian Foundation for Basic Research (grants 03-02-17135), by grant of President of Russian Federation (MK 4586.2004.2). V.B.K. acknowledges Russian Science Support Foundation for financial support.

References

[1] Hodgkin, L. A. and Huley, A.F., *J. Physiol.* **117** *(1952) 500.*

[2] Pinto, R.D., Varona, P., Volkovskii, A.R., Szcs, A., Abarbanel, H.D.I. and Rabinovich, M.I., *Phys. Rev. E* **62** *(2) (2000) 2644.*

[3] Lemasson, G., Lemasson S. and Moulins, M., *Prog. Biophys. Mol. Biol.* **64** *(1995) 201.*

[4] Fitzhugh, R., Impulse and physiological states in models of nerve membrane, *Biophys. J.* **50** *(1961) 445-466.*

[5] J. Nagumo, S. Arimoto and S. Yoshizawa, An active impulse transmission line simulating nerve axon, *Proc. IRE 50 (1962) 2061-2070.*

[6] A. C. Scott. *Neuroscience: A mathematical primer, Springer-Verlag, New York, 2002.*

[7] C. Koch. *Biophysics of computation: Information processing in single neurons, Oxford University Press, Oxford, 1998.*

[8] S. Binczak, V. B. Kasantsev, V. I. Nekorkin, J. M. Bilbault, Experimental study of bifurcations in modified FitzHugh-Nagumo cell, *Electronics Letters* **39** *(2003) 961-962.*

[9] V. B. Kazantsev, Selective communication and information processing by excitable systems, *Phys. Rev. E* **64** *(2001) 056210.*

[10] S. P. Dawson, M. V. D'Angelo and J. E. Pearson, Towards a global classification of excitable reaction-diffusion systems, *Phys. Lett. A* **265** *(2000) 346-352.*

[11] J. Rinzel and B. B. Ermentrout, Analysis of neural excitability and oscillations, In *Methods in neuronal modeling, C. Koch and I. Segev editors, second edition, MIT press, Cambridge, Massachusetts (1998) 251-292.*

[12] H. Korn and P. Faure, Is there chaos in the brain ? II. Experimental evidence and related models, *C.R. Biologies* **326** *(2003) 787-840.*

[13] J.C. Magee, Trends Neurosci. **26** (1), 14 (2003); O. Melamed *et al.* Trends Neurosci. **27** (1), 11 (2004).

[14] K. Yoshino, T. Nomura, K. Pakdaman, and S. Sato, Phys. Rev. E **59**, 956 (1999); K. Pakdaman, Phys Rev E **63**, 041907 (2001).